Preprints of the 19th World Congress
The International Federation of Automatic Control
Cape Town, South Africa. August 24-29, 2014

Integration of fault diagnosis and control by finding a trade-off between the detectability of stochastic fault and economics

Yuncheng Du, Hector Budman, Thomas Duever

Department of Chemical Engineering, University of Waterloo, Waterloo, Ontario, Canada, N2L 3G1
(e-mail: hbudman@uwaterloo.ca, tom.duever@uwaterloo.ca)

Abstract: This paper presents a first principle model based methodology for simultaneous optimal tuning of a fault detection algorithm and a feedback controller. The key idea is to calculate the effect of stochastic input disturbances on the variability of the output variables by using a generalized polynomial chaos (gPC) expansion and a mechanic model of the process. A two-level optimization is proposed for simultaneously tuning the fault detection and controller algorithms. The goal of the outer level optimization is to find a trade-off between the efficiency for detecting faults and the closed loop performance, while the inner optimization is designed to optimally calibrate the fault detection algorithm. The proposed method is illustrated for a continuous stirred tank reactor (CSTR). The results show that the computational cost of the gPC-based method is significantly lower than a Monte Carlo (MC) simulation-based approach, thus demonstrating the potential of the gPC method for dealing with large problems.

Keywords: Fault detection and control, polynomial chaos, economic impact

1. INTRODUCTION

Most fault detection and diagnosis (FDD) systems are implemented at the supervisory level on top of the control system. Thus, naturally fault detection approaches are based on variables, which are also used for feedback control. While there is a large body of literature on FDD (Zufiria, 2012, Dong, et al., 2012), the issue of integration of control and diagnostic algorithms has not been addressed as much. A key challenge for integrating FDD and process control is that they often have competing objectives. For instance, when process control is very accurate, the corresponding controlled variable deviates little from the setpoint while FDD requires sufficiently large deviations for effective detection (Davoodi, et al., 2013, Meng & Yang, 2012). Methods have been proposed for optimal simultaneous tuning of FDD and control based on robust norms (Jacobson & Nett, 1991, Scott, et al., 2013), but these are often conservative since they are based on worst-case scenarios or deterministic linear model. To avoid linearization and reduce conservatism, standard statistical monitoring charts have been used, but these studies were limited to simple deterministic faults (Bin Shams, et al., 2011). Compared with Monte Carlo (MC) simulations based uncertainties analysis, a power series and polynomial chaos expansions were used to propagate uncertainties onto states and outputs, which in general saves computational time (Nagy & Braatz, 2007).

The current work addresses the problem of optimal simultaneous tuning of a FDD and controller in the presence of stochastic disturbances by using gPC expansions of inputs and outputs. A significant reduction in computational effort is observed by using the gPC method as compared with MC based-approach. The topics addressed in this work are as follow:

(1) The tuning parameters of the closed loop controller and/or control setpoint are optimized to achieve an optimal trade-off between FDD efficacy and closed-loop performance.

(2) The generalized polynomial chaos (gPC) expansion and Galerkin projections are used to quantify the variability in controlled and manipulated variables resulting from stochastic faults entering the system in the form of input disturbances. A non-isothermal continuous stirred tank reactor (CSTR) system is used as case study.

(3) Numerical tests are conducted to verify the ability of the proposed method to design a fault detection/controller combination that is both efficient for detecting faults and for maintaining good closed loop performance.

This paper is organized as follows. In section 2, the theoretical background on gPC is presented. The optimization problems formulated for simultaneously tuning the fault detection algorithm and the controller are given in section 3. An endothermic continuous stirred tank reactor (CSTR) is introduced as a case study in section 4. Analysis and discussion of the results are presented in section 5 followed by conclusions in section 6.

2. QUANTIFICATION OF VARIABILITY IN OUTPUTS IN RESPONSE TO RANDOM INPUTS USING gPC

The objective is to quantify the effect of stochastic inputs on different output variables (states), which are described by a system of ordinary differential equations (ODEs). The generalized polynomial chaos (gPC) method (Xiu, 2010) has been proposed for approximating the states of a system with random inputs by polynomial descriptions from the Wiener-Askey family. A variable, x, is represented as a polynomial chaos expansion:

$$x(\omega)=\sum_{i=1}^{\infty} a_i \Phi_i(\xi(\omega)) \quad (1)$$

, where $\omega \in \Omega$ is an element in the event space, Φ_i is a polynomial from an orthogonal Wiener-Askey family, ξ is a random vector and $\{a_i\}$ are estimated as explained below. Generally, (1) is truncated with a finite number of random variables and a finite expansion order. The total number of terms N in a complete polynomial chaos expansion of an arbitrary order p for a response function having n uncertain inputs, is given by

$$N = 1 + P = (n+p)!/n!\,p! \quad (2)$$

To calculate the coefficients a_i, a method referred to as intrusive approach is used (Tagade & Choi, 2013), where the gPC representations of the stochastic variables are explicitly substituted into the model. For simplicity the following single variable (u) problem with operator ℓ and input term κ is studied

$$\ell(u, t; \omega) = \kappa(t; \omega) \quad (3)$$

,where ℓ is a differential operator in the time variable t. The random influence $\boldsymbol{\omega}$ is assumed to be parameterized by finite independent random variables $\boldsymbol{\xi} = \{\xi_1, \xi_2, \ldots, \xi_n\}$. Then, the solution u to a particular differential equation is expanded into a polynomial chaos expansion

$$u(t;\xi)=\sum_{i=1}^{P} u_i(t)\Phi_i(\xi(\omega)) \quad (4)$$

,where $\{u_i(t)\}$ are the gPC coefficients and $\{\Phi_i(\xi(\omega))\}$ are multi-dimensional orthogonal polynomials in terms of ξ. By substituting (4) into (3):

$$\ell\left(\sum_{i=1}^{P} u_i \Phi_i, t; \xi\right) \approx \kappa(t;\xi) \quad (5)$$

Then, a Galerkin projection is employed to obtain a coupled system of ($P+1$) equations by multiplying both sides of each polynomial basis by $\{\Phi_j(\xi(\omega))\}_{j=1}^{P}$, which yields

$$\left\langle \ell\left(\sum_{i=1}^{P} u_i \Phi_i, t; \xi\right), \Phi_j \right\rangle \approx \left\langle \kappa, \Phi_j \right\rangle \quad (6)$$

,where $j=1,\ldots,P$. Once the coefficients of the expansion are obtained, it is possible to compute the statistics of the solution with the following formulae:

$$E(u) = E[\sum_{i=0}^{p} u_i \Phi_i] = u_0 E[\Phi_0] + \sum_{i=0}^{p} E(\Phi_i) = u_0 \quad (7)$$

$$\mathrm{var}(u) = E[(u - E(u))^2] = E[(\sum_{i=1}^{P} u_i \Phi_i - u_0)^2]$$
$$= E[(\sum_{i=1}^{P} u_i \Phi_i)^2] = E[u_i^2 E(\Phi_i^2)] \quad (8)$$

Also, the probability density function (PDF) of the solution is approximated by sampling samples from the distribution of $\boldsymbol{\xi}$ and substituting these samples into (4).

3. METHODOLOGY

The simultaneous optimal tuning of a controller and a fault detection algorithm is formulated as a two-level optimization problem composed of an inner level where the fault detection algorithm is calibrated with simulated noisy data and an outer level where optimal tuning parameters of the controller and setpoint are calculated. The inner optimization is explained below followed by the two-level optimization formulation.

3.1 Inner Optimization: Optimal calibration of fault detection algorithm

The faults in the current work are unmeasured disturbances consisting of stochastic perturbations superimposed on a ML-PRS (Multilevel pseudo random signal) as shown in Fig. 1. The objective of the fault detection algorithm is to detect the mean values of the input ML-PRS (e.g. 5 different levels in Fig. 1) from noisy measured values of manipulated and/or controlled variables of the control system.

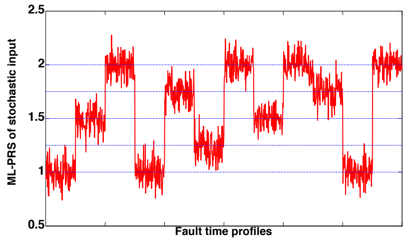

Fig. 1 Fault time profiles representing an intermittent stochastic input fault

In the absence of noise, the PDFs of variables that can be measured and used for detection (u), e.g. manipulated and controlled variables of the closed-loop system can be calculated with the method described in section 2. In reality, due to noise, the PDFs have to be calibrated using actual process data. To calibrate the PDFs using noisy data, an inner optimization problem is formulated about each mean value of the inlet disturbance shown in Fig. 1 as follows:

$$\min_{\lambda_{inner}} J = \sum_{i=1}^{n} (\vartheta_{1,i} - \upsilon_{1,i})^2 + \sum_{i=1}^{n} (\vartheta_{2,i} - \upsilon_{2,i})^2 \quad (9)$$

where $\vartheta_{1,i}$ and $\vartheta_{2,i}$ are the mean and variance of a particular variable of the problem, u, to be used for detection. These means and variances can be calculated numerically with (7) and (8) using the gPC method given in section 2, and are functions of the stochastic input shown in Fig. 1. The terms $\upsilon_{1,i}$ and $\upsilon_{2,i}$ are the mean value and variance of the noisy measurements of u, λ_{inner} is a vector consisting of the mean and variance of the inlet disturbance (fault), and n is the number of the manipulated and/or controlled variables utilized to calibrate the model. Due to the presence of noise, the mean and variance of the input disturbance defining λ_{inner} and calculated from (9) will deviate from the actual values. From λ_{inner}, it is possible to calculate the gPC coefficients for the variables u. Using these coefficients, the PDFs for u's are estimated by substituting random samples into the resulting gPC expansions.

For simplicity, in the current study transient data related to transitions between different mean values in the input as shown in Fig. 1 are ignored and fault detection is performed only when the system reached steady state around each of the mean values of the input. Also, depending on the size of the stochastic perturbations around the mean values of the input disturbance a particular measurement can be found within different PDFs corresponding to different mean values of the disturbance with different probabilities. The maximum probability is used to infer the mean value of the input.

The calibration of the fault detection algorithm can be summarized as follows. (a) Generate a ML-PRS as shown in Fig. 1 and simulate the dynamic model with noise in output variables (b) Compute the expectation and variance of the simulated output variables to be used for detection when the system is operated around each mean value of the input. (c) Around each mean value of the ML-PRS signal solve problem (9) by applying the gPC method outlined in section 2 and by also using the expectation and variance calculated from the noisy signal in item (b) of this procedure. (d) Generate PDFs of manipulated or controlled variables around each mean value of the input shown in Fig. 1.

3.2 Two-level Optimization: Integration of control and fault detection problem

In this section, an algorithm is proposed to simultaneously tune a stochastic fault detection algorithm and a closed loop controller. Since the tuning of the controller affects the detectability of the fault as well as the variability in the manipulated and controlled variables, optimal tuning of control parameters and/or setpoint at which the system should be operated is estimated from an outer optimization problem. A two-level optimization problem is defined as follows:

$$\begin{aligned} &\min_{\lambda_{outer}} J = \mu_1\gamma_1 + \mu_2\gamma_2 + \mu_3\gamma_3 + \mu_4\gamma_4 + \mu_5\gamma_5 \\ &s.t. \quad \text{Problem} \quad (9) \\ &\qquad g_j(k_p, \tau_i) > 0 \quad (j = 1, \cdots, N_{con}) \end{aligned} \tag{10}$$

, where γ_1 is the cost of product quality related variables, γ_2 is the cost associated with variability in controlled variables, i.e. deviations about product quality, γ_3 is the operating costs of the process, e.g., cost of utilities, γ_4 is the cost related to the variability in manipulated variables, i.e. deviation of control actions around nominal operating values and γ_5 is the cost of unobservable faults. λ_{outer} is a vector of decision variables, namely, the tuning parameters of the controller and the setpoint and the subscript *outer* indicates that (10) is the cost of the outer level optimization whereas the inner level is given by (9). Inequality constraints in (10) are imposed to ensure linear stability. The weight coefficients, $\{\mu_i\}$, decide the contribution of each term to the objective function.

The variabilities in objective function (10) account for the competing objectives between costs related to the controller and the cost incurred due to lack of detection of potential faults (γ_5 in (10)). An implicit simplifying assumption made in this work is that an unobservable fault only occurs when the measurements values used for detection correspond to measurements located in the overlap regions of adjacent PDFs calculated as described in section 3.1, since most misclassification will happen near the class boundaries. Thus, γ_5 is numerically calculated as the total area of overlap between the PDFs.

The proposed optimization problem (10) proceeds as per the following steps. (a) Assume initial guesses for the controller parameters and setpoint. (b) Determine stability constraints from a linearized gPC model by using the Routh stability criterion. (c) Calculate the area of overlap of the training sets (PDFs) generated by the inner optimization (9). (d) Minimize the objective function in (10) with respect to λ_{outer}.

A detailed flowchart summarizing the procedure is given in Fig. 2. It should be noticed that if the setpoint of the controlled variable is used as a decision variable in the outer optimization and the problem is nonlinear which directly affects the approximation of the PDFs profile in the inner optimization problem (9).

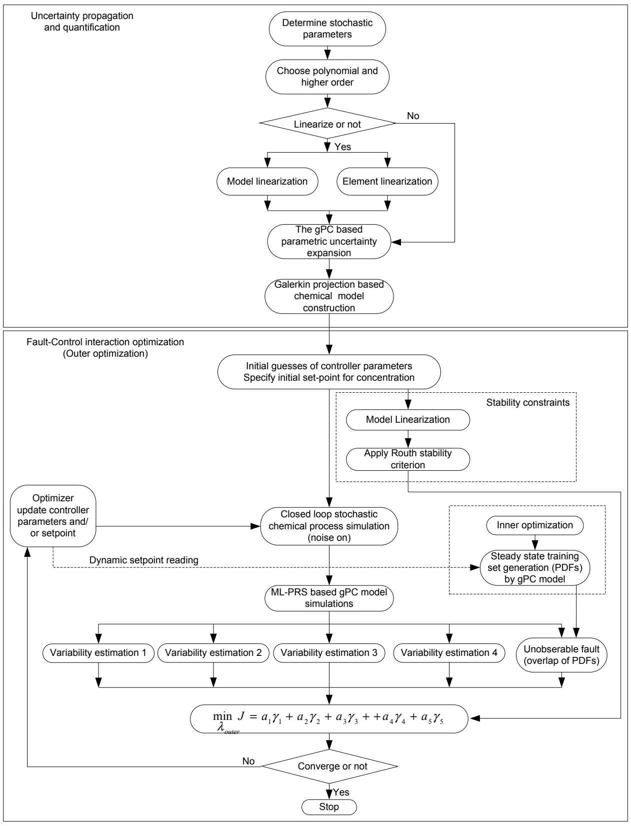

Fig. 2 Flowchart to evaluate the economic significance of unobservable fault

4. CASE STUDY

The proposed methodology is applied to a non-isothermal CSTR system. The mathematical model of the process and a PI controller are described by three ODEs as follows:

$$\begin{aligned} &V_r\,(dC_A/dt) = F/\rho(C_{A0} - C_A) - V_r k_0 C_A \exp(-E/RT) \\ &V_r \rho C_v (dT/dt) = FC_p(T_0 - T) - V_r \Delta H k_0 C_A \exp(-E/RT) + Q \\ &dQ/dt = k_p((F/V_r\rho)(C_{A0} - C_A) - V_r k_0 C_A \exp(-E/RT)) \\ &\qquad - k_p/\tau_i\,(C_{A,set} - C_A) \end{aligned} \tag{11}$$

, where k_p and τ_i are the controller gain and integral time constant, respectively. The controller is used to control the exit reactant concentration C_A by manipulating the external heat Q. The fault detection algorithm seeks to identify changes in the mean of the inlet reactant concentration C_{A0} from measured values of the manipulated variable Q. It should be noticed that only the output heat is employed in this study for fault detection, since the outlet concentration shows smaller variability. However in principle both can be used for detection, but this is beyond the scope of the current work. The inlet concentration C_{A0} changes as shown in Fig. 1. The parameter settings used for the CSTR simulation are given in (Bin Shams, et al., 2011). The objective is to solve problem (10) to find optimal tuning parameters for the *PI* controller and the optimal setpoint for C_A subject to proper training of the fault detection algorithm according to (9).

5. RESULTS AND DISCUSSION

5.1 Model formulation by gPC expansion

The application of Galerkin projection requires integrating the differential equations with respect to an appropriate selection of a polynomial for a particular random variable. Using the orthogonality property of the basis functions, these integrations are possible when dealing with polynomial terms. However, the integration of non-polynomial terms, e.g., the Arrhenius expression in (11) is not straightforward. This problem is addressed in this work by approximating the Arrhenius term with a 2^{nd} order Taylor series expansion. A normally distributed uncertainty is assumed and a Hermite polynomial is used to perform the proposed approximation.

To verify the accuracy of the approximation of the Arrhenius term by the Taylor expansion, the solution of the problem with the gPC model is compared to MC simulations. The comparison was conducted for the same operating conditions as listed in (Bin Shams, et al., 2011). The variance of the stochastic inlet concentration around a mean value used for this comparison is 0.1 gmoles/L.

For the gPC-based solution, the PDF profiles in outlet concentration are calculated by sampling from the random event and substituting the samples into the gPC solution obtained as outlined in section 2. The maximum, minimum and mean of solutions at each time instant are recorded. For the MC simulations, (a) samples of inlet concentration following the same statistical properties are generated, (b) each sample is substituted into the nonlinear CSTR model, and (c) the resulting outlet concentration values are stored for comparison. As shown in Fig. 3, the black dotted line is the deterministic response of nonlinear CSTR (only the mean value on inlet concentration is considered). The green lines correspond to 20 randomly chosen samples in MC simulations. These red lines show the results of the gPC solution using the 2^{nd} order Taylor expansion to approximate the Arrhenius term. Comparing with MC simulations, the gPC based solution provides as expected upper and lower bounds on outlet concentration changes. In addition, the key advantage of the gPC model is dramatic reduction in computational time as compared to MC simulations. For a prescribed inlet concentration, the computational time for 10,000 sample of MC simulation is around 3 hours on an Intel$^{@}$ Core^{TM} Duo desktop (2.40 GHz and 4.0 GB RAM). By contrast, the computing time for the gPC method is around 21 seconds, where the same number of random samples is substituted to the gPC PDF expression to approximate the solution at each time instant. This clearly illustrates that the use of gPC model is instrumental for solving the two-level optimization problem in (10), since the problem has to be solved many times during the optimization search thus leading to a dramatic reduction in computational time for the gPC based solution as compared to MC based approach.

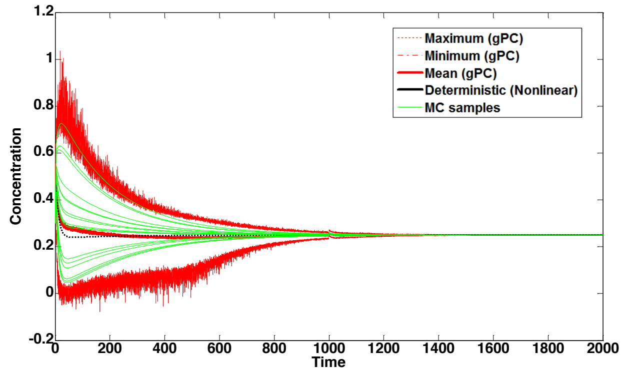

Fig. 3 Simulation results of gPC model, Monte Carlo and deterministic nonlinear model

5.2 Steady state model calibration

As a first step, the fault detection algorithm described in section 3.1 was tested for detecting changes in the expected value of the inlet concentration (of the type shown in Fig. 1) from a set of external heat measurements. 5 mean values in inlet concentration are studied, where the mean varies from 1.0 gmoles/L to 2.0 gmoles/L in steps of 0.25 gmoles/L. Stochastic perturbations are added around these mean values which are assumed to be normally distributed with zero mean and a variance of 0.1 gmoles/L (see Fig. 1). A ML-PRS signal is designed using these mean values and the added stochastic perturbations about them as shown in Fig. 1. Different noise levels in the controlled and manipulated outputs are considered to investigate the effect of the signal to noise ratio on the optimization and the fault detection efficiency.

Table 1 lists the results of the fault detection algorithm calibrated as per the optimization in (9) for a 1% measurement noise level, where the Hermite polynomial is used and the highest order of the polynomial is 2. For the ML-PRS, the L is the maximum length of the sequence and m is the number of measurements in each sequence.

In Table 1, $\bar{C}_{A0}^{Simu}$ is the known value used in simulations, $\bar{C}_{A0}^{Opt}$ and ζ^{Opt} are the values calculated from the solution of problem (9). The optimization problem was solved with 500 and 2000 samples, respectively. As seen, the number of measurements in each sequence shows a great influence on the optimal results. For example, for 500 measurements, some cases failed to converge to the right values. This is because when fewer measurements are used, the transients during changes between mean values become dominant whereas the gPC solution of the model is obtained for simplicity by assuming steady state. Also, as explained before, the expectation and mean of the input resulting from (9) are not identical to the actual values because of noise.

Table 1. Comparison of two inner optimization strategies

$\bar{C}_{A0}^{Simu}$	L=124, m=2000		L=124, m=500	
	$\bar{C}_{A0}^{Opt}$	ζ^{Opt}	$\bar{C}_{A0}^{Opt}$	ζ^{Opt}
1.0	1.0534	0.1410	1.2713	0.1170
1.25	1.2757	0.1207	1.3720	0.1086
1.50	1.5039	0.1057	1.5111	0.1023
1.75	1.7357	0.0955	1.6867	0.0983
2.0	1.9695	0.0891	1.8667	0.0953

Once the gPC model is constructed, the PDFs of the external heat duty, obtained at different expected values of the inlet concentration, can be obtained. The PDFs are shown in Fig. 4, where the horizontal axis is the external heat duty, and the vertical axis is the normalized probability. A fault class to be identified by the fault detection algorithm is referred to by the expected value of inlet concentration. For instance, *"class: 1.0"* means the mean of inlet concentration is 1.0 gmoles/L.

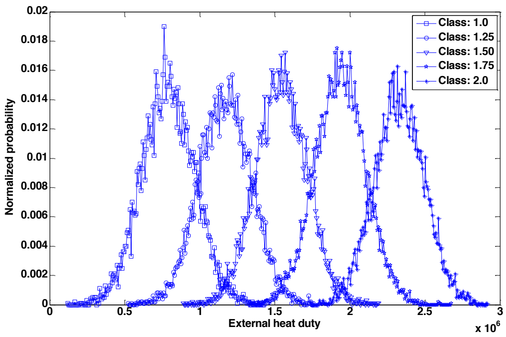

Fig. 4 PDFs of 5 classes on inlet concentration

5.3 Optimal tuning of controller

A first case study consisted in solving (10) described in section 3.2 for optimizing only the tuning parameters of the controller namely, k_p and τ_i. The objective was to test whether the optimally tuned controller can reduce the combined cost associated with loss due to variability in concentration, heat and unobservable faults.

Table 2 shows results of the optimum controller parameter and the cost of the objective function defined in (10), where the set point of outlet concentration is fixed at 0.25 gmoles/L. The resulting controller parameters were found to be similar to the ones reported by (Bin Shams, et al., 2011), where only a deterministic square wave fault was studied. However in contrast to the previous work of Bin Shams et al. it was found that, due to the stochastic perturbations around the means considered in the current work, the costs for the largest or smallest values of inlet concentrations have higher cost. An explanation is that the tuning parameters of the controller try to minimize the overlaps between the PDFs corresponding to different inlet concentrations shown in Figure 4. This is achieved at the cost of introducing greater variabilities in product quality and operating costs in objective function (10), since the controller tries to shift the corresponding PDFs far apart from each other. The resulting overlap, as measured by the total area of overlapping of PDFs, is given in Table 2. As seen, the total overlap is smaller with the optimized tuning parameters of the controller as compared to the non-optimized ones used by Bin-Shams et al, 2011 (k_p=75508 and τ_i =0.507).

As expected, the cost defined in Problem (10) with the non-optimized tuning of controller parameters is higher than the optimum obtained from the solution of (10). For example, the value of cost function with the optimized tuning parameters has decreased by around 17%, from 16.427 to 13.612, when the mean value of inlet concentration is 1.0 gmoles/L.

Table 2. Summary of the results for outer optimization

$\bar{C}_{A0}^{Simu}$	J^{non}	k_p^{opt} [cal/s/gmol]	τ_i^{opt} [s]	J^{opt}	Overlaps Before	Overlaps After
1.00	16.427	81521.50	0.566	13.612	1.259	1.125
1.25	14.943	20175.84	0.082	12.233	1.361	1.084
1.50	13.657	19034.54	0.172	11.523	1.360	1.086
1.75	14.904	99773.78	0.340	12.136	1.318	1.171
2.00	15.831	14709.06	0.547	12.830	1.218	0.938

5.4 Optimal tuning of controller and set point

A second study was conducted where the setpoint of outlet concentration was chosen as an additional decision variable along with the tuning parameters of the controller to minimize the cost function in (10). Table 3 shows the optimum results of decision variables, the related cost and the normalized overlaps area between the PDFs of the heat input.

Table 3. Summary of the results for outer optimization

$\bar{C}_{A0}^{Simu}$	k_p^{opt} [cal/s/gmol]	τ_i^{opt} [s]	Set point	J^{opt}	Overlaps Before	Overlaps After
1.00	41375.12	1.304	0.498	8.978	1.263	0.552
1.25	83835.62	1.595	0.365	8.790	1.365	0.950
1.50	82061.19	1.697	0.348	8.501	1.322	0.904
1.75	69635.40	1.075	0.378	8.804	1.329	0.809
2.00	130554.09	1.242	0.362	9.912	1.245	0.786

Compared with Table 2, the value of the objective function is smaller. For instance, the cost in (10) at an inlet concentration of 1.0 gmoles/L has been decreased by 34%, from 13.612 to 8.978, when the set point is also used as a decision variable. In addition, the overlap in each optimization was monitored. As expected, the overlap areas are smaller as compared to the result without the optimization of the setpoint.

5.5 Fault identification results and comparison with MC

The efficiency of the fault detection algorithm embedded in the two-level optimization problem solved in section 5.4 was also tested for efficacy. Table 4 shows fault identification rate for different noise levels in external heat measurements using the gPC-based solution.

Table 4. Summary of the results for fault identification

$\overline{C}_{A0}^{Simu}$	noise level [%]					
	1		3		10	
	No.	Rate	No.	Rate	No.	Rate
1.00	76	0.924	173	0.827	232	0.768
1.25	93	0.907	146	0.854	189	0.811
1.50	87	0.913	88	0.912	209	0.791
1.75	84	0.916	118	0.882	211	0.789
2.00	72	0.928	213	0.787	223	0.777
Average	/	0.918	/	0.852	/	0.787

In Table 4, there are 1000 test measurements for each inlet concentration level, and *No.* means the number of samples that were wrongly detected in each level. It is worth mentioning that only one steady state heat measurement was used for each test. The average misdetection rate increases as expected when the noise level increases. Finally, the MC simulations of the nonlinear CSTR model were used with non-optimal tuning controller parameters (k_p=75508 and τ_i =0.507) to test the detection efficiency as compared to the optimized case. The MC simulations were used in this case to rule out any possible inaccuracy related to the use of a gPC-based solution. Table 5 shows the fault identification results.

Table 5. Summary of the results for fault identification

$\overline{C}_{A0}^{Simu}$	noise level [%]					
	1		1		10	
	No.	Rate	No.	Rate	No.	Rate
1.00	231	0.769	246	0.754	256	0.744
1.25	239	0.761	253	0.747	261	0.739
1.50	221	0.779	235	0.765	292	0.708
1.75	150	0.850	163	0.837	235	0.765
2.00	93	0.907	108	0.892	146	0.854
Average	/	0.813	/	0.799	/	0.762

For MC simulations, 10,000 samples are used to generate the PDF profiles. The average fault identification rate is 81.3%, as shown in Table 5, which is approximately 10% lower, as compared to the result in Table 4 for the first noise level. In addition, the detection rate decreases as the noise levels increase. This further confirms that the proposed method for simultaneously tuning the controller and the fault detection algorithm results in improved detection.

6. CONCLUSIONS

In the present work, a methodology has been developed to simultaneously optimize closed loop performance and fault detection efficiency. The proposed approach is tested for an endothermic continuous stirred tank reactor (CSTR). The main novelty of the proposed approach is that it permits to address the effect of stochastic inputs on the outputs by using gPC approximations and the process model. The use of gPC is shown to be instrumental because the variabilities of the input and output variables can be quickly calculated using analytical expressions. Since these variabilities have to be calculated repeatedly during the optimization search the dramatic reduction in computation time with gPC as compared to MC simulations makes this approach especially attractive for solving the simultaneous optimal tuning and fault detection problem for large systems.

REFERENCE

Bin Shams, M., Budman, H. & Duever, T., 2011. Finding a trade-off between obervability and connomics in the fault detection of chemical processes. Computers and Chemical Engineering, pp. 319-328.

Davoodi, M., Golabi, A., Talebi, H. A. & Momeni, H., 2013. Simultaneous fault detection and control design for switched linear systems based on dymamic oberver. Optimal Control Applications and Methods, 34(1), pp. 35-52.

Dong, J., Verhaegen, M. & Gustafsson, F., 2012. Robust Fault Detection with Statistical Uncertainty in Identified Parameters. IEEE Transactions on Signal Processing, 60(10), pp. 5064-5077.

Jacobson, C. & Nett, C. N., 1991. An integrated approach to controls and diagnosis using the four parameter controller. IEEE Control Systems, 11(22), pp. 22-28.

Meng, X. J. & Yang, G. H., 2013. Simultaneous fault detection and control for stochastic time-delay systems. International Journal of Systmes Science, pp. 1-12.

Nagy, Z. & Braatz, R. D., 2007. Distributional uncertainty analysis using power series and polynomial chaos expansions. Journal of Process Control, Volume 17, pp. 229-240.

Riggs, J., 1999. Chemical process control. Texas: Ferret Publishing.

Scott, J. K., Findeisen, R., Braatz, R. D. & Raimodo, D. M., 2013. Design of Active Inputs for Set-Based Fault Diagnosis. Washington, DC, USA, 2013 American Control Conference.

Tagade, P. M. & Choi, H., 2013. A Generalized Polynomial Chaos based Method for Efficient Bayesian Calibration of Uncertainty Computational Models. Inverse Problems in Science and Engineering, pp. 1-25.

Vergara, A. et al., 2005. Optimised Temperature Modulation of Metal Oxide Micro-hotplate Gas Sensors through Multilevel Pseudo Random Sequences. Sensors and Actuators B, Volume 111-112, pp. 271-280.

Xiu, D., 2010. Numerical Methods for Stochastic Computation: A Spectral Method Approach. s.l.:Princeton University Press.

Zufiria, P. J., 2012. A mathematical framework for new fault detection schemes in nonlinear stochastic continuous time dynamical systmes. Applied Mathematics and Computation, Volume 218, pp. 11391-11403.